Coherent correlator and equalizer using a reconfigurable all-optical tapped delay line

Mohammad Reza Chitgarha,[1,*] Salman Khaleghi,[1] Omer F. Yilmaz,[1] Moshe Tur,[2] Michael W. Haney,[3] Carsten Langrock,[4] Martin M. Fejer,[4] and Alan E. Willner[1]

[1]*Department of Electrical Engineering, University of Southern California, Los Angeles, California 90089, USA*

[2]*School of Electrical Engineering, Tel Aviv University, Ramat Aviv 69978, Israel*

[3]*Department of Electrical and Computer Engineering, University of Delaware, Newark, Delaware 19716, USA*

[4]*Edward L. Ginzton Laboratory, Stanford University, Stanford, California 94305, USA*

**Corresponding author: chitgarh@usc.edu*

Received March 11, 2013; revised May 30, 2013; accepted May 31, 2013;
posted May 31, 2013 (Doc. ID 186780); published June 25, 2013

We experimentally demonstrate a reconfigurable optical tapped delay line in conjunction with coherent detection to search multiple patterns among quadrature phase shift keying (QPSK) symbols in 20 Gbaud data channel and also to equalize 20 and 31 Gbaud QPSK, 20 Gbaud 8 phase shift keying (PSK), and 16 QAM signals. Multiple patterns are searched successfully on QPSK signals, and correlation peaks are obtained at the matched patterns. QPSK, 8 PSK, and 16 QAM signals are also successfully recovered after 25 km of SMF-28 with average EVMs of 8.3%, 8.9%, and 7.8%. A penalty of <1 dB optical signal to noise penalty is achieved for a 20 Gbaud QPSK signal distorted by up to 400 ps/nm dispersion.

OCIS codes: (060.2360) Fiber optics links and subsystems; (060.4370) Nonlinear optics, fibers; (190.4223) Nonlinear wave mixing.

http://dx.doi.org/10.1364/OL.38.002271

A key building block of many digital signal processing applications is the tapped delay line (TDL), in which an incoming data stream is tapped at different time intervals, given complex weights, and then added together [1]. Two important applications of TDL are the correlation of incoming data symbols to a predetermined pattern and the equalization of distorted signals to undo the effect of transmission impairments [2]. It might be desirable to implement an optical TDL to perform all-optical correlation and pattern recognition as well as equalization to potentially improve the levels of tunability, bandwidth, and reconfigurability.

Optical TDLs (OTDLs) using differential delays and multiple taps have been demonstrated using the following: fixed fiber-based delays, planar lightwave circuits (PLCs), fiber Bragg grating arrays, and connected Mach–Zehnder interferometers (MZIs) in which each MZI represents two taps of the TDL [3–6]. Recently, noncoherent correlators and equalizers on differential quadrature phase shift keying (DQPSK) signal have been demonstrated [7].

Given the importance of higher-order modulation formats in coherent optical communication, e.g., phase shift keying (PSK) and quadrature amplitude modulation (QAM) formats, a laudable goal would be to achieve all-optical and data-format-transparent equalizers to decrease the processing load in a coherent receiver. Moreover, taking advantage of both intensity and phase information using coherent detection, correlation on higher-order modulation formats with higher processing capacity and correlation gain can potentially be achieved.

In this Letter, we demonstrate a tunable and reconfigurable OTDL in conjunction with coherent detection first to implement a coherent correlator to simultaneously search multiple patterns among quadrature phase shift keying (QPSK) symbols, and second to realize an all-optical equalizer to equalize QPSK, 8 PSK, and 16 QAM signals after distorting them with chromatic dispersion. The OTDL is demonstrated by implementing an all-optical fan out stage to create multiple replicas of the original signal using $\chi^{(2)}$ nonlinear processes in the periodically poled lithium niobate (PPLN) waveguide, conversion/dispersion delay to induce relative delays on signal replicas [8], and coherent multiplexing in another PPLN waveguide [9]. Multiple patterns are searched successfully on QPSK signals, and correlation peaks are obtained at the matched patterns. We also successfully recovered QPSK, 8 PSK, and 16 QAM signals after 25 km transmission through SMF-28 with average error vector magnitudes (EVMs) of 8.3%, 8.9%, and 7.8%, respectively. Less than 1 dB optical signal to noise ratio (OSNR) penalty is achieved for a 20 Gbaud QPSK signal distorted by up to 400 ps/nm dispersion.

The conceptual block diagram of the coherent OTDL is shown in Fig. 1. At the first stage, the original signal, along with multiple dummy pump lasers (λ_{Di}) and a continuous wave (CW) pump (λ_{p1}), is injected into a PPLN waveguide with quasi-phase matching (QPM) wavelength of λ_{QPM}. The signal and a CW pump laser, which are located symmetrically around the $\omega_{\mathrm{QPM}} = c/\lambda_{\mathrm{QPM}}$ (c is the speed of light), mix through the sum frequency generation (SFG) process to produce a signal copy at 2 ω_{QPM}. The SFG term then mixes with multiple dummy pump lasers ($\omega_{Di} = c/\lambda_{Di}$) through the difference frequency generation (DFG) process to create signal copies at $\omega_{Ci} = 2 \times \omega_{\mathrm{QPM}} - \omega_{Di}$ [7]. At the second stage, a spatial light modulator (SLM) is utilized to write the complex weights on the signal replicas. The tap amplitudes can be tuned by varying dummy pump powers, whereas the tap phases can be changed by varying the SLM phases. Subsequently, these replicas are sent through a chromatic dispersive element to induce wavelength-dependent delays on the signal copies at the next stage. The relative delay between two adjacent replicas can be obtained by $\tau = D \times \Delta\lambda$, where D is the dispersion parameter and $\Delta\lambda$ is the wavelength separation between

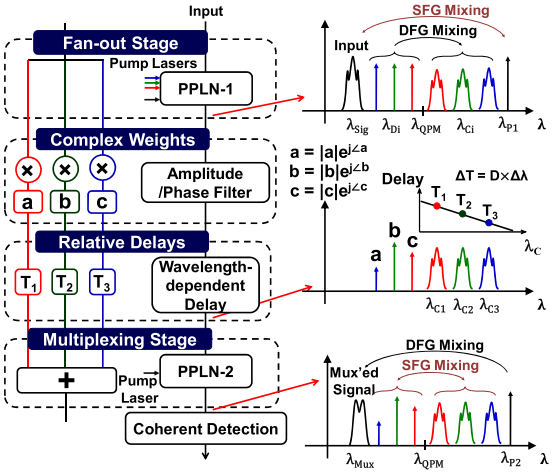

Fig. 1. Conceptual block diagram of a reconfigurable OTDL that includes four stages: fan-out, complex weights, relative delays, and multiplexing.

two replicas. Therefore, tap delays can be continuously tuned by varying dummy pump wavelengths. These weighted and delayed signal copies are equivalent to OTDL taps which need to be coherently combined. In the multiplexing stage, each delayed signal copy at $\lambda_{Ci} = c/\omega_{Ci}$ mixes with its reused dummy pump at λ_{Di} through SFG, and creates a signal at 2 ω_{QPM}. Another pump laser at λ_{P2} is also injected to the second PPLN, with the same QPM wavelength waveguide for the DFG process to multiplex these signals in λ_{Mux}.

To realize an equalizer, the relative delay needs to be set at the half-symbol duration. The weights of the OTDL depend on the transfer function of incoming data distortion. It is also possible to perform multicasting of equalized signal by introducing multiple CW pumps in the second PPLN.

To realize a coherent correlator, the delay needs to be set to the symbol duration. Figure 2 shows how coherent detection can be used to achieve a high-performance correlator. To identify the appearance of four particular consecutive values [a, b, c, d] in a long pattern of QPSK symbols, the correlator weights need to be set to the phase conjugate of the target pattern, i.e., [a*, b*, c*, d*]. An N-tap correlator on QPSK signal has an output of $(n+1)^2$ QAM constellation. Figure 2(b) shows how

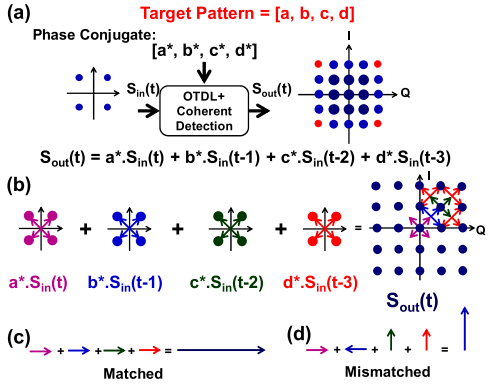

Fig. 2. Coherent correlator (a) input versus output constellation for 4 tap QPSK correlators. (b) 25 QAM contellation can be generated by combining 4 QPSK signals (c) matched to the target pattern, and (d) mismatched to the target pattern.

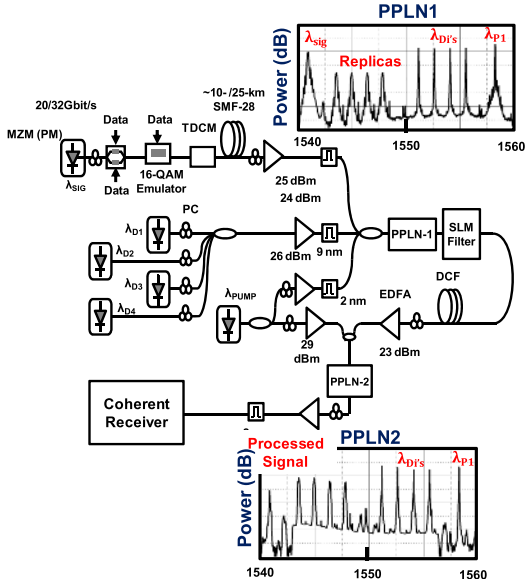

PM: Phase Modulator
MZM: Mach-Zehnder Modulator
DCF: Dispersion Compensating Fiber
PC: Polarization Controller
DLI: Delay Line Interferometer
BPF: Bandpass Filter

Fig. 3. Experimental setup for coherent optical correlator/equalizer. The fan-out and multiplexing stages are done in PPLN1 and PPLN2, respectively.

25 QAM constellation can be generated by 4 QPSK signals. The corner points, i.e., upper right, upper left, lower left, and lower right, which are indicated by red color in Fig. 2(a), correspond to [a, b, c, d], $j \times [a, b, c, d]$, $-1 \times [a, b, c, d]$, and $-j \times [a, b, c, d]$, respectively, while other constellation points correspond to other 4-symbol patterns. Therefore, by sending the result to the coherent receiver, each pattern is mapped to one constellation corner point due to their different phases which can potentially be used to recognize simultaneously all four patterns with the same correlation weights. One example of matched pattern (corresponding to upper right corner) and one example of mismatched pattern are shown in Figs. 2(c) and 2(d), respectively.

The experimental setup for the coherent correlator/equalizer is shown in Fig. 3. A nested Mach–Zehnder modulator is used to generate the input 62 and 40 Gbit/s QPSK data [pseudorandom bit sequence (PRBS) $2^{31} - 1$] at ~1541.440 nm. The resulting signal is sent to a phase modulator to generate 8 PSK signals 60 Gbit/s or a 16 QAM emulator to emulate 80 Gbit/s 16 QAM signal. A tunable dispersion compensation module (TDCM), along with two SMF-28 fibers with 10 and 25 km lengths, is employed to emulate dispersion on the input signal. The input signal is amplified, filtered, and sent to a 4 cm PPLN waveguide (PPLN-1) along with an amplified pump laser at ~1560.75 nm. Four dummy pump lasers (λ_{D1-4}) are coupled together, amplified, and launched to the first PPLN waveguide. The QPM wavelength of the waveguide is set to ~1550.7 nm by temperature tuning. SFG and DFG processes will create multiple replicas of the input signal at different wavelengths. The output of the PPLN-1 is sent to a SLM-based programmable filter used to filter the dummy pump lasers and the generated signal copies, and to control the phases of the pump lasers prior to the second wavelength conversion stage. The filtered pumps

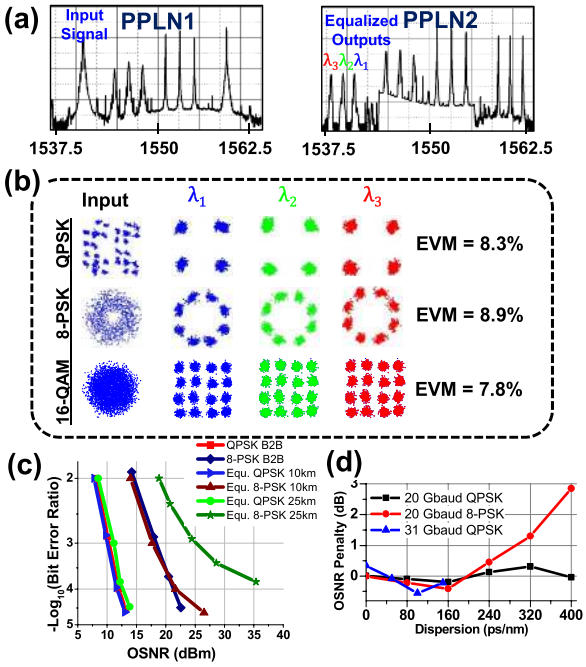

Fig. 4. Coherent equalizer results with three taps. (a) optical spectra of PPLN-1 and PPLN-2 outputs. (b) 16 QAM, 8 PSK, and QPSK distorted signal with 25 km SMF-28 transmission before and after equalization on 3 different wavelengths. (c) BER measurements and (d) OSNR penalty for different amount of dispersion.

and the signals are then sent through a ~180 or 390 m DCF (for correlator or equalizer, respectively) in order to induce the relative delays. Next the dummy pump lasers and the signal copies are amplified and sent to a 5 cm PPLN waveguide (PPLN-2) with QPM ~1550.7 nm to multiplex OTDL taps coherently. The output signal is then filtered and sent to the coherent receiver to capture the constellation and bit error rate (BER) measurements. We noted that there is polarization sensitivity in PPLN waveguides which requires controlling of the incoming polarization state. In order to perform correlation and equalization on polarization-multiplexed signals, a polarization diversity technique can be utilized [10].

Figure 4 illustrates the optical equalizer performance with three taps. Figure 4(a) shows optical spectra of PPLN-1 and PPLN-2 outputs when three equalized copies are generated at λ_1, λ_2, and λ_3. The in phase and quadrature (IQ) constellation diagrams of the transmitted 20 Gbaud QPSK, 8 PSK, and 16 QAM signals through 25 km of SMF-28 fiber are shown in Fig. 4(b). The signals are equalized and multicast to three different wavelengths. Figure 4(b) also depicts these output constellations on the right. A clean IQ constellation is obtained for each copy after equalization with average EVMs of ~8.3%, 8.9%, and 7.7%, respectively. BER measurements are performed on back to back as well as equalized 20 Gbaud QPSK and 8 PSK signals after 10 and 25 km of SMF-28 transmission in Fig. 4(c). The performance of the equalizer is evaluated in terms of OSNR penalties by emulating various amounts of dispersion using the TDCM on 20 and 31 Gbaud QPSK and 20 Gbaud 8 PSK signals in Fig. 4(d). As can be seen, <1 dB OSNR penalty can be achieved for a 20 Gbaud QPSK signal distorted by up to 400 ps/nm dispersion.

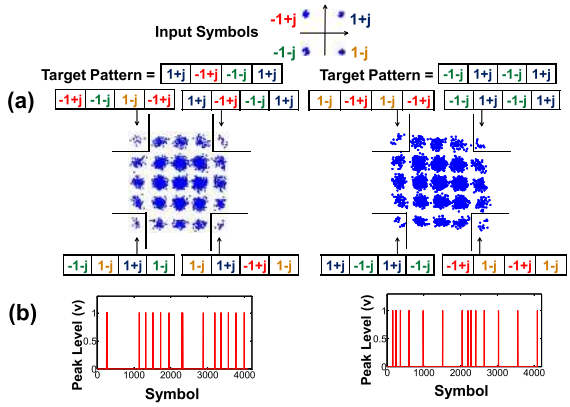

Fig. 5. Coherent correlator results with four taps. (a) 4-tap correlator outputs for two different target patterns, and (b) correlator peaks corresponding to matched patterns.

Figure 5 shows the coherent correlator results with four taps. The 25 QAM output is shown in Fig. 5(a) for two different patterns with EVMs of 7.2% and 7.5%. As can be seen, all output symbols in all four corner points of the IQ-plane can be detected separately as the target pattern with 0°, 90°, 180°, and –90° rotations. In Fig. 5(b), the correlator peaks on QPSK symbols to the target pattern $[1+j,\ -1+j,\ -1-j,\ 1+j]$ are shown. The pattern $[1+j,\ -1-j,\ 1+j,\ -1-j]$ is searched on the same 1000 QPSK symbols, and its correlation peaks are depicted in Fig. 5(c).

This work was made possible by support from NSF, CIAN, DARPA, and Cisco Systems.

References

1. J. G. Proakis, *Digital Communications* (McGraw-Hill, 2000).
2. S. J. Savory, G. Gavioli, R. I. Killey, and P. Bayvel, Opt. Express **15**, 2120 (2007).
3. B. Moslehi, J. W. Goodman, M. Tur, and H. J. Shaw, Proc. IEEE **72**, 909 (1984).
4. M. S. Rasras, I. Kang, M. Dinu, J. Jaques, N. Dutta, A. Piccirilli, M. A. Cappuzzo, E. Y. Chen, L. T. Gomez, A. Wong-Foy, S. Cabot, G. S. Johnson, L. Buhl, and S. S. Patel, IEEE Photon. Technol. Lett. **20**, 694 (2008).
5. M. C. Hauer, J. E. McGeehan, S. Kumar, J. Touch, J. Bannister, E. R. Lyons, C. H. Lin, A. A. Au, H. P. Lee, D. S. Starodubov, and A. E. Willner, J. Lightwave Technol. **21**, 2765 (2003).
6. C. R. Doerr, S. Chandrasekhar, P. J. Winzer, A. R. Chraplyvy, A. H. Gnauck, L. W. Stulz, R. Pafchek, and E. Burrows, J. Lightwave Technol. **22**, 249 (2004).
7. S. Khaleghi, O. F. Yilmaz, M. R. Chitgarha, M. Tur, N. Ahmed, S. Nuccio, I. Fazel, X. Wu, M. W. Haney, C. Langrock, M. M. Fejer, and A. E. Willner, IEEE Photon. J. **4**, 1220 (2012).
8. Y. Dai, Y. Okawachi, A. C. Turner-Foster, M. Lipson, A. L. Gaeta, and C. Xu, Opt. Express **18**, 333 (2010).
9. M. R. Chitgarha, S. Khaleghi, O. F. Yilmaz, M. Tur, M. W. Haney, C. Langrock, M. M. Fejer, and A. E. Willner, *Optical Fiber Communication Conference*, OSA Technical Digest (Optical Society of America, 2012), paper OTh4H.
10. H. Hu, R. Nouroozi, R. Ludwig, B. Hüttl, C. Schmidt-Langhorst, H. Suche, W. Sohler, and C. Schubert, J. Lightwave Technol. **29**, 1092 (2011).